Pharmacological Research 179 (2022) 106193

Contents lists available at ScienceDirect

Pharmacological Research

journal homepage: www.elsevier.com/locate/yphrs

Dietary lipid droplet structure in postnatal life improves hepatic energy and lipid metabolism in a mouse model for postnatal programming

Tomas Jelenik [a,b,1,2,3], Andrea Kodde [c,1,4], Dominik Pesta [a,b,d,e,f,1,5], Esther Phielix [g,6], Annemarie Oosting [c], Elisabeth Rohbeck [a,b], Bedair Dewidar [a,b,h], Lucia Mastrototaro [a,b], Sandra Trenkamp [a,b], Jaap Keijer [i,7], Eline M. van der Beek [j,8], Michael Roden [a,b,k,*,9]

[a] Institute for Clinical Diabetology, German Diabetes Center, Leibniz Center for Diabetes Research at Heinrich-Heine University, Düsseldorf, Germany
[b] German Center for Diabetes Research, Partner Düsseldorf, Germany
[c] Danone Nutricia Research, Utrecht, The Netherlands
[d] Institute of Aerospace Medicine, German Aerospace Center (DLR), Cologne, Germany
[e] Center for Endocrinology, Diabetes and Preventive Medicine (CEDP), University Hospital Cologne, Cologne, Germany
[f] Cologne Excellence Cluster on Cellular Stress Responses in Aging-Associated Diseases (CECAD), Cologne, Germany
[g] Department of Nutrition and Movement Sciences, School for Nutrition and Translational Research in Metabolism, Maastricht University Medical Center, Maastricht, The Netherlands
[h] Department of Pharmacology and Toxicology, Faculty of Pharmacy, Tanta University, Tanta, Egypt
[i] Human and Animal Physiology, Wageningen University, Wageningen, The Netherlands
[j] Department of Pediatrics, University Medical Centre Groningen, University of Groningen, Groningen, The Netherlands
[k] Department of Endocrinology and Diabetology, Medical Faculty and University Hospital, Heinrich-Heine University, Düsseldorf, Germany

ARTICLE INFO

Keywords:
Early life programming
Mitochondrial function
Supramolecular structure of lipid droplets
Milk fat globule membrane
Insulin resistance
Diacylglycerol

ABSTRACT

Early-life diets may have a long-lasting impact on metabolic health. This study tested the hypothesis that an early-life diet with large, phospholipid-coated lipid droplets (Concept) induces sustained improvements of hepatic mitochondrial function and metabolism. Young C57BL/6j mice were fed Concept or control (CTRL) diet from postnatal day 15 (PN15) to PN42, followed by western style (WSD) or standard rodent diet (AIN) until PN98. Measurements comprised body composition, insulin resistance (HOMA-IR), tricarboxylic acid (TCA) cycle- and β-oxidation-related hepatic oxidative capacity using high-resolution respirometry, mitochondrial dynamics, mediators of insulin resistance (diacylglycerols, DAG) or ceramides) in subcellular compartments as well as systemic oxidative stress. Concept feeding increased TCA cycle-related respiration by 33% and mitochondrial fusion protein-1 by 65% at PN42 (both p 0.05). At PN98, CTRL, but not Concept, mice developed

Abbreviations: AIN, American Institute of Nutrition rodent diet; Concept, concept diet (Nuturis®); cCER, cytoplasmic ceramides; cDAG, cytoplasmic diacylglycerols; CER, ceramides; CETF, electron-transferring flavoprotein complex; CSA, citrate synthase activity; CTRL, control diet; DAG, diacylglycerols; ETC, electron transfer capacity; FCCP, carbonyl cyanide-p-trifluoromethoxyphenylhydrazone; LCR, leak control ratio; mCER, membrane ceramides; mDAG, membrane diacylglycerols; ldCERL, lipid droplet ceramides; ldDAG, lipid droplet diacylglycerols; NAFLD, non-alcoholic fatty liver disease; NEFA, non-esterified fatty acids; OXPHOS, oxidative phosphorylation; PN, postnatal day; RCR, respiratory control ratio; ROS, reactive oxygen species; TBARS, thiobarbituric acid reactive substances; TCA, tricarboxylic acid; WSD, Western style diet.

* Correspondence to: c/o Institute for Clinical Diabetology, German Diabetes Center, Leibniz Institute for Diabetes Research at Heinrich-Heine University, 40225 Düsseldorf, Germany.
E-mail address: michael.roden@ddz.de (M. Roden).
[1] Authors contributed equally.
[2] Current affiliation: TJ is currently an employee of Boehringer-Ingelheim Pharma GmbH & Co. KG, Biberach an der Riss, Germany. EvdB was an employee of Danone Nutricia Research at the time of the study.
[3] ORCID ID: 0000–0002-2061–1162.
[4] ORCID ID: 0000–0001-8692–6864.
[5] ORCID ID: 0000–0002-5089–3586.
[6] ORCID ID: 0000–0001-6188–6528.
[7] ORCID ID: 0000–0002-9720–7491.
[8] ORCID ID: 0000–0002-7923–3653.
[9] ORCID ID: 0000–0001-8200–6382

https://doi.org/10.1016/j.phrs.2022.106193
Received 10 November 2021; Received in revised form 9 March 2022; Accepted 24 March 2022
Available online 28 March 2022

hyperinsulinemia (CTRL/AIN 0.22 ± 0.44 vs. CTRL/WSD 1.49 ± 0.53 nmol/l, p 0.05 and Concept/AIN 0.20 ± 0.38 vs. Concept/WSD 1.00 ± 0.29 nmol/l, n.s.) and insulin resistance after WSD (CTRL/AIN 107 ± 23 vs. CTRL/WSD 738 ± 284, p 0.05 and Concept/AIN 109 ± 24 vs. Concept/WSD 524 ± 157, n.s.). WSD-induced liver weight was 18% lower in adult Concept-fed mice and β-oxidation-related respiration was 69% higher (p 0.05; Concept/WSD vs. Concept/AIN) along with lower plasma lipid peroxides (CTRL/AIN 4.85 ± 0.28 vs. CTRL/WSD 5.73 ± 0.47 μmol/l, p 0.05 and Concept/AIN 4.49 ± 0.31 vs. Concept/WSD 4.42 ± 0.33 μmol/l, n.s.) and were in part protected from WSD-induced increase in hepatic cytosolic DAG C16:0/C18:1. Early-life feeding of Concept partly protected from WSD-induced insulin resistance and systemic oxidative stress, potentially via changes in specific DAG and mitochondrial function, highlighting the role of early life diets on metabolic health later in life.

1. Introduction

The prevalence of childhood obesity keeps increasing [1] and contributes to the global rise in the incidence of type 2 diabetes, cardiovascular diseases and non-alcoholic fatty liver disease (NAFLD) [2,3]. Consumption of hypercaloric fat- and carbohydrate-rich diets contributes to this pandemic, by promoting ectopic lipid deposition, which is related to insulin resistance, and key to the development of type 2 diabetes [4]. Excessive lipid deposition can lead to adaptation of hepatic mitochondrial function as demonstrated in mouse models of insulin resistance, obesity or lipodystrophy [5–7]. In addition, subcellular accumulation of bioactive lipids, such as diacylglycerols (DAG) and ceramides (CER), have a major role in mediating lipid-induced insulin resistance by interfering with the insulin signalling pathway [4]. Both the quantity and quality of dietary lipids affect metabolic function.

Dietary lipids can either exert beneficial metabolic effects, as reported for n-3 polyunsaturated fatty acids- and monounsaturated fatty acids-enriched diets [8,9], or may promote inflammation and insulin resistance, as reported for saturated fats [10]. In addition to these direct effects, dietary lipid quality, particularly during pre- and (early) postnatal life, was shown to have sustained effects on offspring metabolic health. Moreover, a high saturated fat intake during pregnancy impaired insulin sensitivity [11,12], as well as hepatic and skeletal muscle mitochondrial function [13,14] in adult offspring. Interestingly, postnatal dietary modulations can attenuate the metabolic consequences of an adverse maternal diet for the offspring [15]. Postnatal feeding of a diet rich in n-3 long-chain polyunsaturated fatty acids prevented adult adiposity in rodents exposed to an obesogenic environment [16].

Observational studies demonstrated that breastfeeding associates with a reduced risk of overweight and obesity [17,18], and it is postulated that besides fatty acid composition also the physical characteristics of human milk may contribute to these beneficial effects. Lipid droplets of human milk are larger compared to those of infant milk formula and are surrounded by a milk fat globule membrane, consisting of phospholipids, glycolipids, cholesterol and membrane proteins [19,20]. To mimic the supramolecular structure of human milk lipid droplets, an infant milk formula with large lipid droplets, coated with phospholipids (Nuturis®) was developed [21]. Previous studies in mice demonstrated that postnatal feeding with a diet containing Nuturis® (Concept) protects, at least in part, from western style diet (WSD)-induced lipid accumulation, adipocyte hypertrophy and insulin resistance [22,23]. Although the underlying mechanisms remain elusive, there is evidence that Concept may enhance expression of genes regulating mitochondrial content and oxidative function in murine adipose tissue [24]. Of note, current paradigms indicate that adipose tissue dysfunction will alter hepatic energy metabolism, ultimately leading to type 2 diabetes and NAFLD [4].

Hepatic mitochondrial functionality is important for the regulation of lipid metabolism and indeed Concept has been shown to enhance expression of hepatic mitochondrial markers, directly after postnatal exposure, suggesting increased lipid oxidation [25]. However, the long-term effects of the early life Concept exposure on hepatic mitochondrial function, biogenesis and dynamics as well as lipid composition and content has not been investigated. To this end, we examined the effects of postnatal Concept feeding on key features of hepatic mitochondrial function, biogenesis, dynamics, efficiency and oxidative stress, as well as hepatic lipid content and composition (i) after postnatal exposure and (ii) after subsequent exposure to standard chow diet or WSD in adult mice. We hypothesized that early postnatal Concept feeding improves hepatic mitochondrial function and lipid metabolism, thereby protecting from WSD-induced metabolic deterioration later in life.

2. Materials and methods

2.1. Animals

All experiments were performed according to the guidelines for the care and use of animals (GV-SOLAS [Society for Laboratory Animal Science], Freiburg, Germany) and approved by the local council of animal care in line with the requirements of the German Animal Protection Act and compliant to EU Directive 2010/63/EU.

Male (n = 36) and female (n = 36) C57BL/6JOlaHsd breeder mice (9 weeks old at arrival, Envigo, Horst, The Netherlands) were maintained on a 12-h light-dark cycle in standard cages under conventional conditions, regularly checked for pathogens and received all diets and water ad libitum. Upon arrival, breeder mice were housed with 1 per cage (Macrolon type 3 cages, floor area 800 cm^2, height 150 mm, equipped with poplar bedding, nest material made of hemp fibres, wooden blocks for gnawing and red shelter mouse houses), and were allowed to acclimatize for one week, receiving a grain-based diet (2018S, Teklad Global 18% Protein Rodent Diet, Envigo, The Netherlands) as provided by the breeder and subsequently adapted to a semi-synthetic American Institute of Nutrition 93 G (growth) diet (AIN93G, Research Diet Services) [26] for two weeks. Breeders were time-mated (see Supplementary Material for more information) and provided with the AIN93G during breeding, pregnancy and until day 15 of lactation. At PN2, pups were randomly assigned to a dam to reduce between-litter variability and avoid litter effects, and culled to four male and two female pups per dam, except one litter who consisted of three males and three females and another litter which consisted of two males and four females, respectively, due to the sex-ratio and total offspring born. On PN15, dam and litters were assigned to either Concept or CTRL groups and fed with respective diets (see below), while pups were also allowed to drink milk from the dams (Fig. 1).

Concept and CTRL diets were provided daily as a dough on the floor of the cage. After weaning on PN21, male offspring were housed in pairs (with littermate) in Macrolon type 3 cages identical to the breeder mice and continued their respective diets until PN42. At PN42, males were either dissected or switched to an AIN-93M (AIN) diet or to a WSD (20 w/w % fat) challenge until PN98 (Fig. 1). The study comprised the following six groups: PN 42: CTRL (n = 13) and Concept (n = 10) and PN98: CTRL/AIN (n = 10), CTRL/WSD (n = 12), Concept/AIN (n = 12) and Concept/WSD (n = 16) (for power calculation see supplementary material). Group sizes were different as one litter (n = 4 males) was incorrectly assigned to the Concept group, but these 4 animals were kept in the study after consultation with the Animal Welfare Officer, as the animals could not be used for other experiments given their exposure to

the diet. The extra male in the litter with 3 males and 3 females was kept in the study for the same reason and housed with the two littermates until the end of the study. To further reduce litter effects, offspring of the same litter were per pair divided over different groups, i. e. either sacrificed at PN42 or assigned to WSD vs. AIN group.

Body weight was measured twice a week from PN21 onwards, and food intake once a week from PN42 onwards. Food intake was assessed per cage by weighing the metal cage top with food per 24 h. Body composition was monitored by using nuclear magnetic resonance (Whole Body Composition Analyzer; Echo NRI, Houston, Texas, USA) at PN42 and PN98 [27]. All animal procedures were performed in the light phase.

At PN42 or PN98, mice were fasted for 3 h, anesthetized (isoflurane/N_2O/O_2) and killed by cervical incision, while trunk blood was obtained for EDTA plasma. Fresh pieces of liver were immediately transferred to biopsy preservation solution on ice for analysis of mitochondrial function using high-resolution respirometry within 2 h. The remaining tissues were snap-frozen and stored at − 80 °C for later analysis.

2.2. Diets

The postnatal diets are semi-synthetic diets (Research Diets Services), containing 28.2% (w/w) CTRL or Concept infant milk formula (IMF) powder, are iso-caloric and contain similar amounts of macronutrients. To establish appropriate rodent macro- and micronutrient composition according to AIN-93G standards [26] only proteins, carbohydrates, vitamins and minerals were added, i. e. the lipid portions of the diets were entirely derived from the IMFs. The CTRL IMF powder was a commercially available IMF manufactured per good manufacturing practices (ISO 22000) and intended for use of 0–6 months old infants (Danone Nutricia Research, Utrecht, The Netherlands). To produce Concept IMF (Nuturis®, Danone Nutricia Research, Utrecht, The Netherlands), 0.5 g/l milk phospholipid concentrate of bovine origin (Lipamin M20, Lecico, Hamburg, Germany) was added to the recipe and the processing adapted to generate larger lipid droplets surrounded with phospholipids [21,22]. The mode diameter based on volume of the lipid droplet was 3.13 μm for Concept compared to 0.47 μm for CTRL. The composition of the diets is given in Table 1.

Table 1
Dietary composition of the early life diets (g per kg powder).

Diet	Programming diet	
	CTRL	Concept
Carbohydrates	655	655
Sugars[a]	189	189
Polysaccharides[b]	420	420
Protein	203	203
Fat	70	70
Saturated fatty acids	31	31
Monounsaturated fatty acids	27	27
Polyunsaturated fatty acids	12	12
Phospholipids[c]	0.1	1.1
Cholesterol	–	0.03
Fiber	45.2	45.2
Vitamin & mineral mix	45	45

CTRL: control diet; Concept: Concept diet.
[a] Total sugars, including lactose, glucose and sucrose
[b] Including starch and maltodextrin
[c] Phospholipids derived from bovine milk

2.3. Hepatic and skeletal muscle mitochondrial function

Mitochondrial respiration (O_2 flux) and reactive oxygen species (ROS) emission were measured in freshly permeabilized liver and soleus muscle samples using the Oxygraph-2k (Oroboros Instruments, Innsbruck, Austria) as described [28]. Defined respiratory states were obtained by employing the following protocols: (i) TCA-linked respiration, by consecutive addition of 2 mM malate, 10 mM pyruvate (complex I, state 2 respiration also termed as LEAK), 2.5 mM ADP, 10 mM glutamate and (complex I, state 3 also termed as OXPHOS (oxidative phosphorylation)), 10 mM succinate (complex I+II, state 3 (OXPHOS)), 10 μM cytochrome C (mitochondrial membrane integrity check), 5 nM oligomycin (complex I+II, state 4o also termed as LEAKomy), carbonyl cyanide-p-trifluoromethoxyphenylhydrazone (FCCP; stepwise titrations of 0.25 μM up to the final concentration of max. 1.25 μM) in order to obtain maximal electron transfer capacity (ETC) and 2.5 μM antimycin A (non-mitochondrial respiration); as well as (ii) β-oxidation-linked respiration, successive addition of 2 mM malate, 1 mM octanoyl-carnitine (complex I + electron-transferring flavoprotein complex (CETF), state 2 (LEAK)), 2.5 mM ADP (complex I + CETF, state 3 (OXPHOS)), 10 μM cytochrome C, 5 nM oligomycin (complex I + CETF, state 4o (LEAKomy)), FCCP to obtain maximal ETC (stepwise titrations of 0.25 μM up to the final concentration of max. 1.25 μM, state u) and 2.5 μM antimycin A. Addition of cytochrome C did not significantly increase oxygen consumption, indicating integrity of the mitochondrial outer membrane after saponin permeabilization. Respiratory control ratio (RCR), reflecting mitochondrial coupling, was calculated for each protocol from the respective ratio of state 3 (OXPHOS):state 4o (LEAKomy) [28,29]. Leak control ratio (LCR), reflecting mitochondrial proton leakage, was calculated using state 4o (LEAKomy):ETC ratios [28].

Rates of hepatic ROS emission at state 4o were quantified by fluorometric measurement of H_2O_2 concentration by the O2k-Fluorescence module (Oroboros Instruments) as described [30].

Citrate synthase activity (CSA) was assessed spectrophotometrically (Citrate Synthase Assay kit, Sigma-Aldrich, St. Louis, MO).

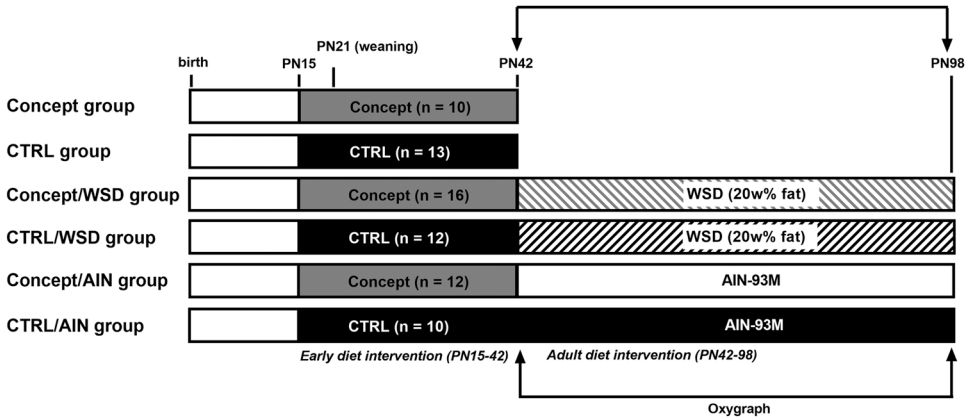

Fig. 1. Study design. Mice were assigned to one of the 6 experimental groups and exposed to either CTRL or Concept diet from PN15 to 42. At PN42, CTRL- and Concept-fed mice were sacrificed and liver tissue was used for respirometry. Mice of the other groups were fed AIN-93M or WSD until PN98. At PN98, remaining mice were sacrificed, and liver tissue was used for respirometry. Body composition was assessed with MRI at PN42 and PN98. AIN: AIN-93M: American Institute of Nutrition rodent diet 93-maintenance, CTRL: control, MRI: magnetic resonance imaging, PN: postnatal day; WSD: western style diet.

Mitochondrial respiration and H_2O_2 emission were normalized for individual CSA values to account for any differences in mitochondrial content.

2.4. Circulating hormones and metabolites

Plasma glucose was measured using the Glucose Assay Kit (Calbiochem®, Merck, KGaA, Darmstadt) and plasma insulin using the Mercodia Mouse Insulin ELISA (Mercodia AB, Uppsala, Sweden). Plasma levels of thiobarbituric acid reactive substances (TBARS), as markers of lipid peroxidation, were measured fluorometrically (BioTek, Bad Friedrichshall, Germany) as reported previously [31]. Plasma non-esterified fatty acid (NEFA) levels were measured using the Free Fatty Acids Kit (Cell Biolabs, INC., San Diego, USA).

2.5. Hepatic lipid analysis

Hepatic triglyceride concentration was measured colorimetrically (Triglyceride Quantification Colorimetric/Fluorometric Kit, BioVision, California, US).

For the rapid and simultaneous quantification of DAG and ceramide species in liver tissue, we used a liquid chromatography triple quadrupole mass spectrometry (LC-MS/MS)-method as deribed before [32]. After immediate freezing of the samples in liquid nitrogen, lipids were extracted and purified from ~50 mg of liver and muscle tissue each. For extraction, fractionation and purification of bioactive lipids, liver tissue was homogenized in 500 µl of buffer A (20 mM Tris/HCL, 1 mM EDTA 0.25 mM EGTA, 250 mM Sucrose, PIC) using an IKA T10 basic Ultra Turrax (IKA; NC, USA) and a tight-fitting glass homogenizer (Wheaton, UK) [32]. Lipids of three subcellular compartment, i e. lipid droplet, cytosol and membrane fractions were obtained by centrifugation. Briefly, samples were transferred to centrifuge tubes, overlaid with 150 µl Buffer A and centrifuged for 1 h, 100,000 * *g*, 4 °C. The floating lipid droplet layer was separated from the underlying cytosol fraction using a slicer (Beckman Coulter, Brea, CA, USA). Subsequently, the cytosol fraction was transferred to a fresh tube, while the membrane fraction remained as a pellet in the centrifuge tube. Internal standards were added and lipids of lipid droplet, cytosol and membrane fraction were extracted according to Folch et al. [33], followed by solid phase extraction (Sep Pak Diol Cartridges; Waters, MA, USA). The resulting lipid phase was dried under a gentle flow of nitrogen, resuspended in 400 µl methanol and then analysed by LC–MS/MS [32]. In brief, the chromatographic separation of analytes was conducted using an Infinity 1290 Ultra-High Performance Liquid Chromatography system (Agilent Technologies Inc., Santa Clara, CA, USA) and a reversed-phase Luna Omega C18 column, 50 × 2.1 mm, 1.6 µm (Phenomenex, Torrance, CA, USA) operated at 50 °C. A binary gradient was used consisting of 5 mM ammonium formate in water (Solvent A) and 5 mM ammonium formate in 90% methanol/10% i-propanol (solvent B) at the flow rate of 0.4 ml/min. The analytes were measured as ammonium adducts (DAGs) or protonated adducts (CERs) using electrospray ionization (ESI) and detected by multiple reaction monitoring (MRM) on a triplequadrupole mass spectrometer (MS, Agilent 6495; Agilent Technologies, CA, USA) operated in positive ion mode.

2.6. Immunoblotting

Immunoblotting of proteins was performed according to a previously described protocol [34]. Proteins were extracted from approximately 30 mg of liver tissue, homogenized in 300 µl of lysis buffer (25 mM trisaminomethane-hydrochloride (Tris-HCl), pH 7.4, 150 mM NaCl, 0.20% Nonidet P-40, 1 mM ethylenediaminetetraacetic acid (EDTA) and 0.1% sodium dodecyl sulfate (SDS), supplemented with a Protease Inhibitor Cocktail and the Phosphatase Inhibitor Cocktail II (Roche, Mannheim, Germany) and loaded onto SDS polyacrylamide gradient gels (4–20% Mini-PROTEAN® TGX™ Precast Protein Gels, Biorad, Hercules, CA, USA). An inter-run calibrator (IRC) was loaded to each gel to account for between-run differences. Prior to immunoblotting, the stain-free gels were UV-activated for 1 min and pictures were taken using the ChemiDoc MP imaging system (Biorad). Proteins were transferred to a polyvinylidene difluoride (PVDF) membrane using the Trans-Blot Turbo Transfer System (Biorad), imaged using the ChemiDoc MP and quantified using Image LabTM 6.0.1 software (Bio-Rad 199 Laboratories) for normalization. The PVDF membrane was blocked with 5% non-fat milk in Tris-buffered saline with Tween 20 (TBST buffer: 10 mM Tris, pH 8.0, 150 mM NaCl, and 0.5% Tween 20) for 2 h at room temperature. Afterwards, the membranes were incubated overnight with primary antibodies at 4 °C and then with horseradish peroxidase (HRP)-conjugated secondary antibodies for 1 h at room temperature. Finally, membranes were coated with Immobilon Western Chemiluminescent HRP Substrate (Merck Millipore, Darmstadt, Germany) and proteins were detected using a ChemiDoc imaging system in combination with the software ImageLab 6.0.1 (Biorad) for densitometric analysis. Data are expressed in arbitrary units and normalized to voltage-dependent anion channel (VDAC) protein to normalize for mitochondrial content. The dynamin related protein (DRP) 1 (5391) and phospho-DRP1 Ser616 (3455) antibodies were purchased from Cell Signaling Technology; peroxisome proliferator-activated receptor gamma coactivator (PGC) 1-α from Millipore (ST1202); mitochondrial transcription factor A (TFAM) from Santa Cruz Biotechnology (sc-166965); other primary antibodies were purchased from Abcam: Mitofusin1 (MFN1) (ab57602), Mitofusin2 (MFN2) (ab56889) and VDAC (ab14734).

Quantitative real-time-PCR (RT-PCR) was performed as described previously [35]. Briefly, total RNA was isolated from 10 mg of frozen liver using the RNeasy Mini Kit (Qiagen, Düsseldorf, Germany), cDNA was transcribed from 1000 ng total RNA with the QuantiTect Reverse Transcription Kit (Qiagen, Cat. No.205311) and used for RT-PCR with QuantiTect SYBR® Green PCR Kit (Qiagen, Cat. No.204145) in a StepOnePlus RT-PCR System (Applied Biosystems, Waltham, MA USA) using QuantiTect Primer Assays (Qiagen, Düsseldorf, Germany). The following primers were purchased from Qiagen: TFAM (QT00154413), PGC1a (QT02524242); hypoxanthine-guanine phosphoribosyltransferase (QT00166768), Peptidylprolyl isomerase A (QT00247709) and β2-microglobulin (QT01149547) were used as endogenous reference genes. Ct values were first normalized to geometric mean of Ct of the 3 reference genes, then to Ct of IRC to obtain the expression fold-change following the ΔΔCt method [35]. A melting curve was created to ensure primer specificity. Each sample was measured in triplicate.

2.7. Calculations and statistics

As a surrogate of insulin resistance, HOMA-IR was calculated from 3-h fasting insulin (mlU/l) * fasting glucose (mmol/l)/22.5 [36,37].

Statistical analyses were performed using GraphPad Prism (8.0.0) except for changes in body weight and body composition over time, which were analysed using SPSS (19.0.0). Data are expressed as mean ± SEM. The effects of early-life diet (Concept vs. CTRL) at PN42 were compared using the unpaired t-test. At PN98, effects of the early (Concept vs. CTRL) and adult diet (AIN vs. WSD) and the interaction between those, were analysed using two-way ANOVA and Sidak's multiple comparisons test in case of an overall early or adult diet effect. Data was tested for normal distribution by the Kolmogorov-Smirnov test and when data did not show a Gaussian distribution, analysed with a Mann-Whitney or Kruskall-Wallis test. Changes in body weight and body composition over time were analysed using repeated measure ANOVA. Differences were considered significant when $p < 0.05$, $p < 0.01$ and $p < 0.001$.

3. Results

3.1. Direct effects of postnatal Concept feeding at PN42

The direct effects of the early-life dietary intervention, as defined by the 4 weeks from PN15 to PN42, were studied at PN42. Body weight was similar between Concept and CTRL (Fig. 2A). However, Concept fed mice had a higher lean body mass (Fig. 2B), while total body fat mass tended to be lower compared to CTRL ($p = 0.06$). Consequently, relative body fat mass was lower after Concept feeding compared to CTRL (Fig. 2C, D).

The differences in body composition did not affect organ weights (Supplementary Table 1).

In the liver, maximum uncoupled TCA cycle-linked respiration was 33% higher ($p = 0.05$) after Concept feeding compared to CTRL (Fig. 3A). No differences were observed for other parameters of TCA-cycle-linked respiration, including LCR and RCR (Supplementary Fig. 1A, B). The parameters of β-oxidation-linked respiration, including LCR and RCR and CSA activities did not differ between Concept and CTRL (Fig. 3B, C, Supplementary Fig. 1C, D). Also, hepatic mitochondrial ROS production, expressed as H_2O_2 emission, was similar between both groups (Fig. 3D). Mitochondrial function and content as well as oxidative stress of the soleus muscle were not different between groups (Supplementary Fig. 2A-D).

Protein content of the biomarkers of mitochondrial biogenesis, PGC-1α and TFAM, was not different between Concept and CTRL at PN42 (Fig. 4A, B). However, there was a 65% increase in MFN1 protein, indicating higher mitochondrial fusion after Concept feeding ($p = 0.03$) (Fig. 4C, D). DRP1 protein and the ratio of DRP1 to phospho-DRP1 (Ser616), as biomarkers of mitochondrial fission, were not different between the groups (Fig. 4E, F).

After 3 h of fasting, there were no differences in plasma glucose, insulin, HOMA-IR, as well as plasma TBARS and NEFA (Supplementary Fig. 3A-F). Liver weight and liver triglycerides were comparable between Concept and CTRL at PN42 (Fig. 5A, B). Cytoplasmic DAGs (cDAG), lipid droplet DAGs (ldDAG) and most membrane DAGs (mDAG) as measured in liver tissue, were not affected by Concept compared to CTRL. However, C20, C22 and C24 mCER were higher in Concept compared to CTRL mice (Fig. 5C and Supplementary Fig. 4A-E).

3.2. Effects of postnatal Concept feeding in adult mice

At PN98, the effect of the early-life feeding with Concept vs CTRL was assessed upon a WSD challenge. Compared to AIN, WSD exposure increased body weight and lean mass over time (PN42–98) to a similar extent in the Concept/WSD and CTRL/WSD groups, also when corrected for the respective baseline values (Fig. 6A, B and Supplementary Figure 5A, B). Concept/WSD showed a somewhat lower increase in (relative) body fat mass over time than CTRL/WSD, which was statistically different compared to CTRL/WSD, when corrected for baseline values (Fig. 6C, D and Supplementary Fig. 5C and D). Neither early nor adult diets affected fasting plasma glucose and NEFA levels (Fig. 6E, I). Plasma insulin and HOMA-IR significantly worsened in CTRL/WSD compared to CTRL/AIN, but not in Concept/WSD compared to Concept/AIN (Fig. 6F-G). Plasma TBARS levels were increased in CTRL/WSD compared to CTRL/AIN, but not in Concept/WSD mice (Fig. 6H).

Compared to AIN, WSD increased hepatic TCA cycle-linked state 3 (succinate) respiration to a similar extent in the Concept/WSD and CTRL/WSD mice (Fig. 7A), while LCR and RCR remained unchanged by WSD and early life diet (Supplementary Fig. 6A, B) at PN98. WSD similarly increased different states of β-oxidation-linked respiration and RCR in Concept/WSD and CTRL/WSD (Fig. 7B, Supplementary Fig. 6D), while LCR remained unaffected and was not different between groups (Supplementary Fig. 6C). WSD, however, increased maximal (FCCP) β-oxidation-linked uncoupled respiration only in Concept/WSD and was 69% ($p = 0.05$) higher compared to Concept/AIN (Fig. 6B). Finally, mitochondrial content, as assessed by CSA, was lower in CTRL/WSD than CTRL/AIN (Fig. 7C). Mitochondrial oxidative stress was reduced by WSD as compared to the restrictive AIN diet (Fig. 7D). There were no group-differences when oxidative stress levels were normalized to CSA (Fig. 7E). Soleus muscle mitochondrial function and content as well as oxidative stress were not different between CTRL/AIN, CTRL/WSD,

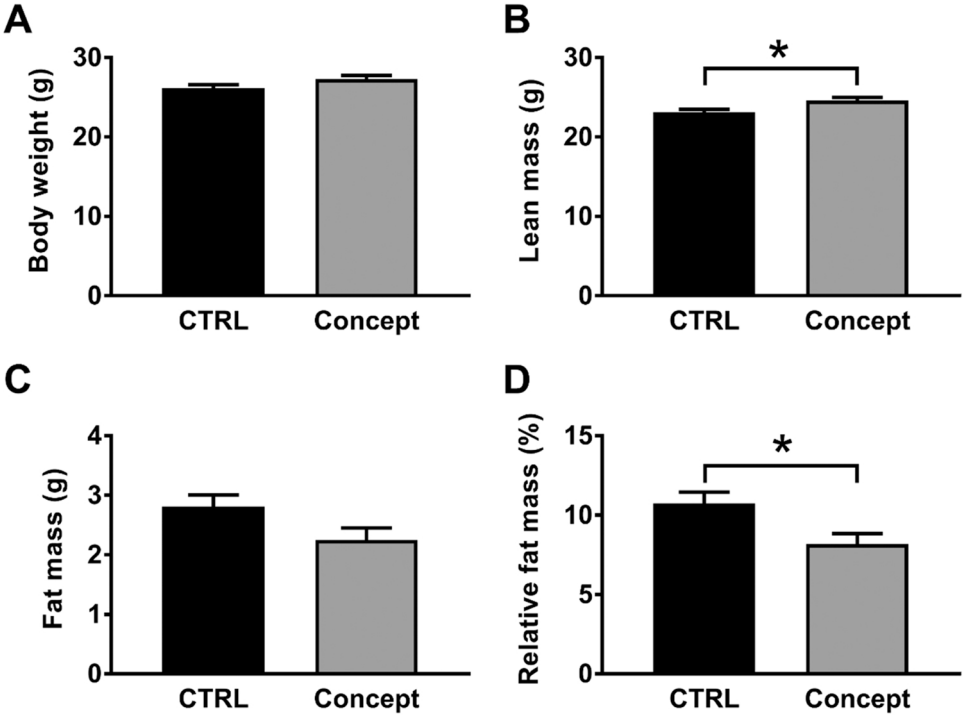

Fig. 2. Direct effects of Concept vs CTRL on body weight and body composition. (A) Body weight at PN42. (B-D) Body composition at PN42. Data are shown as mean ±SEM, CTRL: n = 13; Concept: n = 10. Unpaired t-test; *p < 0.05. CTRL: control.

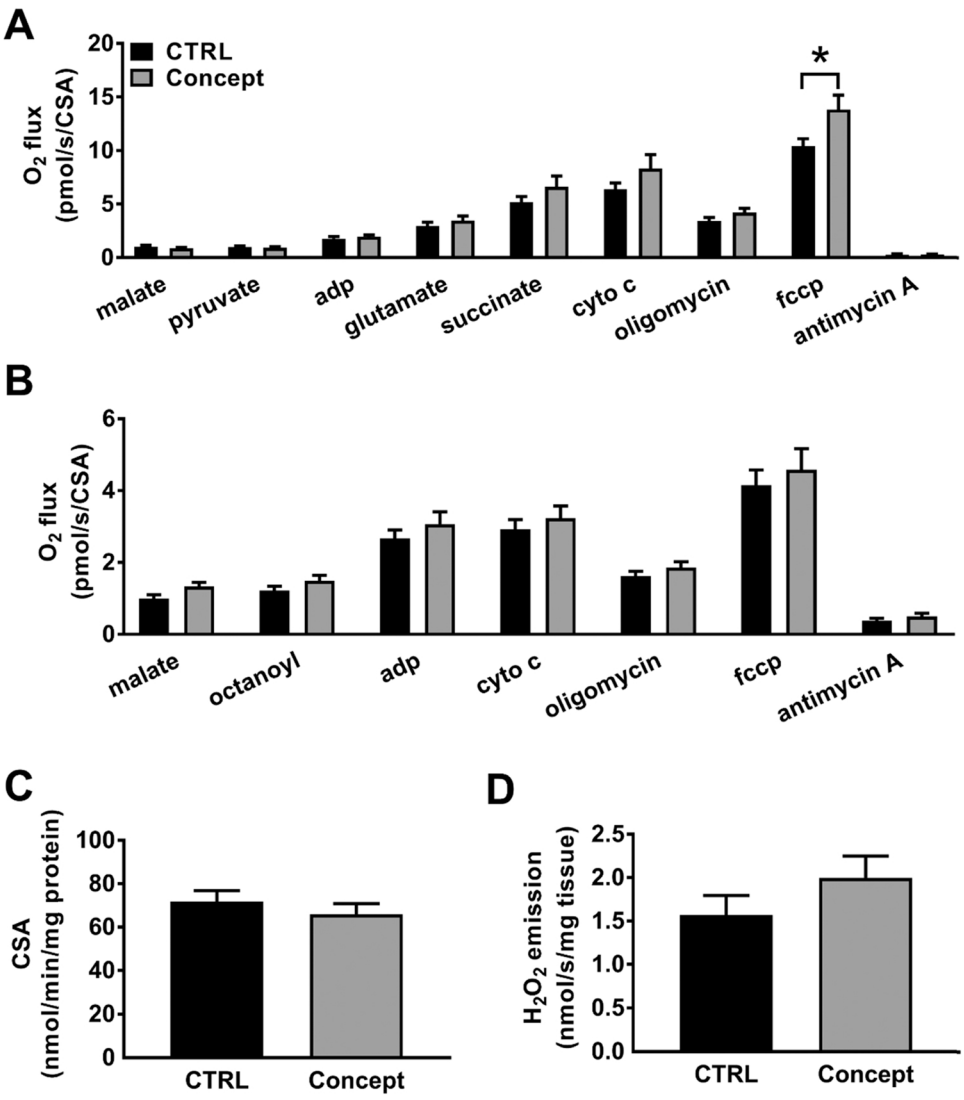

Fig. 3. Direct effects of the Concept diet on mitochondrial function of the liver at PN42. Mitochondrial respiration [O_2 flux normalized to CSA] was measured with substrates supporting TCA cycle (A) and β-oxidation (B). Mitochondrial content (C) was assessed by CSA normalized to protein concentration. Oxidative stress (D) was measured as the rate of malate-stimulated H_2O_2 emission. Data are shown as mean±SEM, CTRL: n = 13; Concept: n = 10. Multiple t-test (A, B) or unpaired t-test (C,D); *p < 0.05. CSA: citrate synthase activity, CTRL: control; cyto C: cytochrome c; fccp: carbonyl cyanide-p-trifluoromethoxyphenylhydrazone; TCA: tricarboxylic acid.

Concept/AIN, and Concept/WSD (Supplementary Fig. 7A-D).

In order to assess long-term effects of postnatal Concept feeding on mitochondrial biogenesis and dynamics, we assessed protein levels of PGC-1α, TFAM, MFN1, MFN2, DRP1 and the ratio of DRP1 to phospho-DRP1 (Ser616). Neither early nor adult diets affected these biomarkers of mitochondrial biogenesis and dynamics (Fig. 8A-F) or the differences of the mitochondrial protein between PN42 and PN98 (Supplementary Fig. 8A-F).

In contrast to CTRL/WSD, liver weight of the Concept/WSD group did not increase upon WSD challenge and was lower compared to that of CTRL/WSD (Fig. 9A). The WSD-induced increase in weight of any other tissue or organ studied was not affected by the early-life Concept diet (Supplemental Table 2). Hepatic triglyceride levels increased upon WSD feeding in both the CTRL/WSD and the Concept/WSD (Fig. 9B). When assaying subcellular fractions to study bioactive lipids in more detail, we found that the WSD challenge increased hepatic cDAG and mDAG species containing C18:1 mainly in CTRL/WSD compared to CTRL/AIN, which only reached significance for cDAG C16:0/C18:1 (Fig. 9C, D and Supplementary Fig. 9A, C, E). Neither the WSD, nor the early Concept feeding had an effect on CER species in the different subcellular fractions (Supplementary Fig. 9B, D and F).

3.3. Correlation analyses

Energy expenditure can best be correlated to lean mass [38], due to significant weight contribution but low metabolic activity of white adipose tissue [39]. Indeed, at PN98, the lean body mass of CTRL groups (CTRL/AIN and CTRL/WSD together) correlated to hepatic mitochondrial respiration from different substrates (Malate $r = 0.490$; Octanoyl-carnitine $r = 0.436$; Oligomycin $r = 0.476$; Antimycin $r = 0.453$; $p < 0.05$ for all; Supplementary Table 3). However, in Concept fed groups, no such correlations were found. As for AIN and WSD animals at PN98, we observed a correlation between lean body mass and respiration rate after ADP ($r = -0.548$), cytochrome c ($r = -0.523$) and FCCP titration ($r = -0.403$), $p < 0.05$ for all (Supplementary Table 4).

4. Discussion

This diet intervention study showed that early-life exposure to a diet comprising large, phospholipid-coated lipid droplets (Concept) affects various features of mitochondrial function and lipid metabolism in rodent liver, but not skeletal muscle. Concept feeding not only directly enhanced maximum hepatic TCA-cycle-linked mitochondrial oxidative capacity and mitochondrial fusion at PN42, but also potentiated β-oxidation-linked oxidative capacity later in life, at PN98. Furthermore,

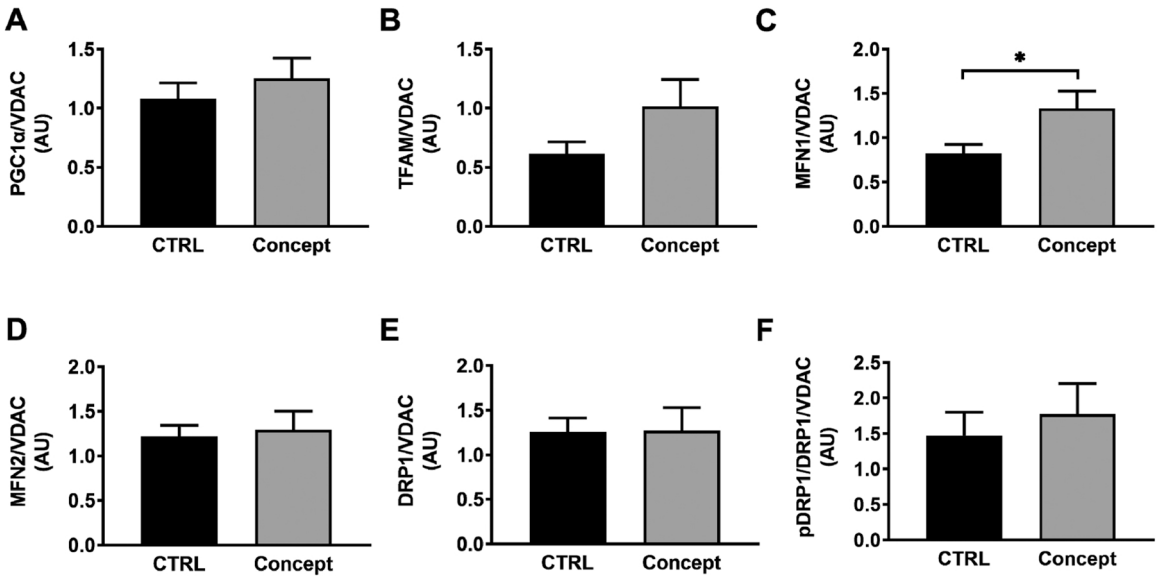

Fig. 4. Direct effects of Concept and CTRL on protein markers of mitochondrial biogenesis and dynamics at PN42. PGC-1α (A), TFAM (B), MFN1 (C), MFN2 (D), DRP1 (E) and pDRP1/DRP1 (F). Data are shown as mean±SEM, CTRL: n = 13; Concept: n = 10. Unpaired t-test. CTRL: control; PGC-1α: peroxisome proliferator-activated receptor gamma coactivator 1-α; TFAM: mitochondrial transcription factor A; MFN1 or 2: mitofusion 1 or 2; DRP1: dynamin-related protein 1, VDAC: voltage-dependent anion channel.

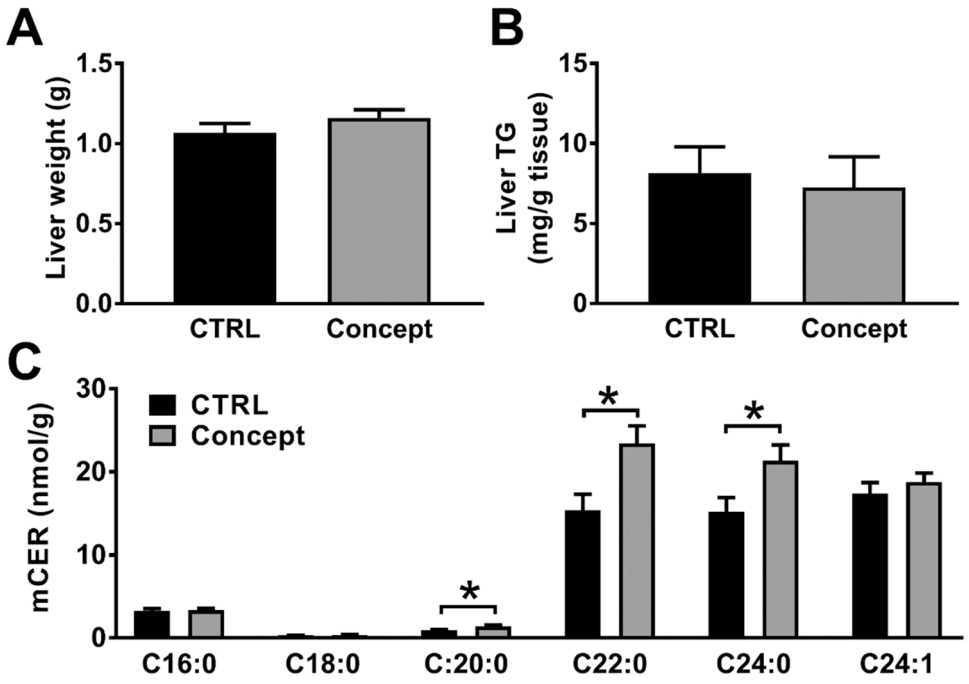

Fig. 5. Direct effects of Concept and CTRL on liver weight and hepatic lipids at PN42. Liver weight (A), liver TG (B) and mCER (C). Data are shown as mean±SEM, CTRL: n = 13; Concept: n = 10 for liver weight; CTRL: n = 12; Concept: n = 10 for liver TG and mCER. Unpaired t-test. CTRL: control; mCER: ceramides in membranes, TG: triglycerides.

postnatal exposure to the Concept diet at least partially protected against WSD-induced hyperinsulinemia, insulin resistance, body fat accumulation, cytosolic and membrane DAG accumulation and systemic oxidative stress.

Early-life environment can affect metabolic health and specifically liver function either adversely, e. g. by foetal over- or undernutrition [40,41], or beneficially, e. g. by breastfeeding [42]. Several rodent and piglet studies suggested that altered hepatic mitochondrial function and ROS production may be associated with this so-called programming of metabolic health [13,43,44]. In those studies, intrauterine growth restricted piglets [43] and rodents born to obese dams [13,44] showed reduced hepatic mitochondrial content, oxidative capacity and increased production of ROS and/or expression of its markers. Early-life feeding with the Concept diet for several weeks increased maximum uncoupled TCA-cycle-linked respiration directly after exposure and maximum uncoupled β-oxidation-linked respiration later in WSD-fed adult mice. These findings suggest that the Concept diet induces programming of hepatic mitochondrial function, increasing maximum oxidative capacity. Interestingly, in the current study, hepatic mitochondrial ROS emission remained unchanged between Concept/WSD

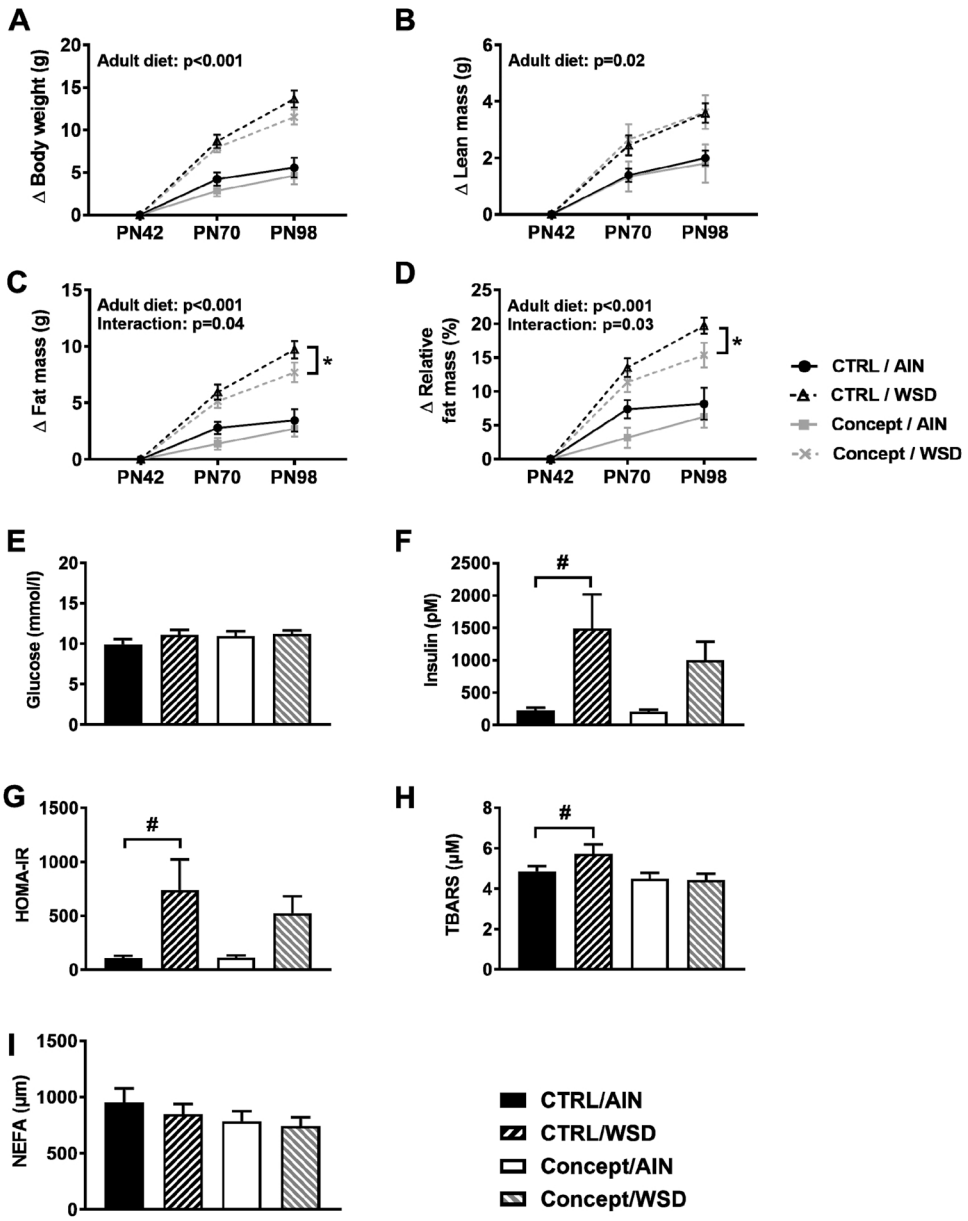

Fig. 6. Long-term effects of postnatal Concept feeding on changes in body weight, body composition and glucose metabolism. Development of body weight (A), lean mass (B), fat mass (C) and relative fat mass (D, % of body weight) from PN42 to PN98 as corrected for baseline. Fasted (3 h) plasma glucose (E), plasma insulin (F), HOMA-IR (G) TBARS (H), and NEFA (I). Data are shown as mean±SEM, CTR/AIN: n = 10; CTRL/WSD: n = 12; Concept/AIN: n = 12; Concept/WSD: n = 16, except for the glucose, HOMA-IR which had n = 9 for the CTRL/AIN and n = 11 for the Concept/AIN. For body weight and composition, repeated measures ANOVA with two factors (early and adult diet) was used and in case of existing interaction between factors, separate factors were tested. *$p < 0.05$ Concept/WSD different from CTRL/WSD. Glucose and insulin data were tested with two-way ANOVA. #$p < 0.01$ WSD effect in groups fed the same early-life diet. AIN: American Institute of Nutrition rodent diet; CTRL: control; NEFA: non-esterified fatty acids; PN: postnatal day; TBARS: thiobarbituric acid reactive substances; WSD: western style diet.

and CTRL/WSD, while plasma lipid peroxides (TBARS) increased only in CTRL/WSD, but not in Concept/WSD. The absence of a rise in ROS production in the face of higher oxidative capacity hints at an improved antioxidant activity and/or altered lipid metabolism, maybe due to preferred β-oxidation or decreased VLDL secretion from the liver of Concept/WSD mice.

Mitochondrial dynamics, i. e. fission and fusion events, are closely related to intact mitochondrial function. One of the factors contributing to NAFLD development is the inadequate mitochondrial quality control [45]. While mitochondrial fusion positively correlates with oxidative phosphorylation capacity [46], mitochondrial fission has a role in the development of hepatic steatosis and metabolic deterioration [47,48]. The present study found evidence for higher mitochondrial fusion upon normalization to mitochondrial content in mice receiving Concept during early life, supporting the contention of an association with the improvement of mitochondrial function in these mice [46]. While there were no long-term effects of postnatal Concept feeding on liver-specific mitochondrial biogenesis and dynamics, we cannot exclude longer-lasting effects on hepatic metabolism, maybe occurring via epigenetic alterations associated with fetal programming [49].

Fat droplets of concept diet are composed of a mixture of phospholipids, proteins and cholesterol, mimicking largely the structure and composition of human fat globules [50]. Although exact mechanisms are still under investigation, the specific structure of Concept may enhance intestinal lipolysis and postprandial lipemia in a way that postprandial responses and bioavailability of ingested fatty acids exert possible longer-term consequences on hepatic bioenergetics.

The WSD intervention increased hepatic oxidative capacity from several mitochondrial substrates. Recent studies demonstrated that hepatic mitochondria can adapt their activity to short-term as well as long-term changes of substrate availability. Specifically, increased lipid availability leads to adaptive increases in mitochondrial oxidative capacity, indicating “mitochondrial flexibility” in both humans and murine obesity, at least during the early course of NAFLD [29]. In the present study, the Concept/WSD mice featured higher hepatic mitochondrial function from different substrates independent of WSD-induced changes in lean body mass, in line with a sustained effect of early life Concept exposure. This effect is likely not related to improved mitochondrial biogenesis, as Concept did not affect hepatic CSA, reflecting mitochondrial content or mass. Collectively, these

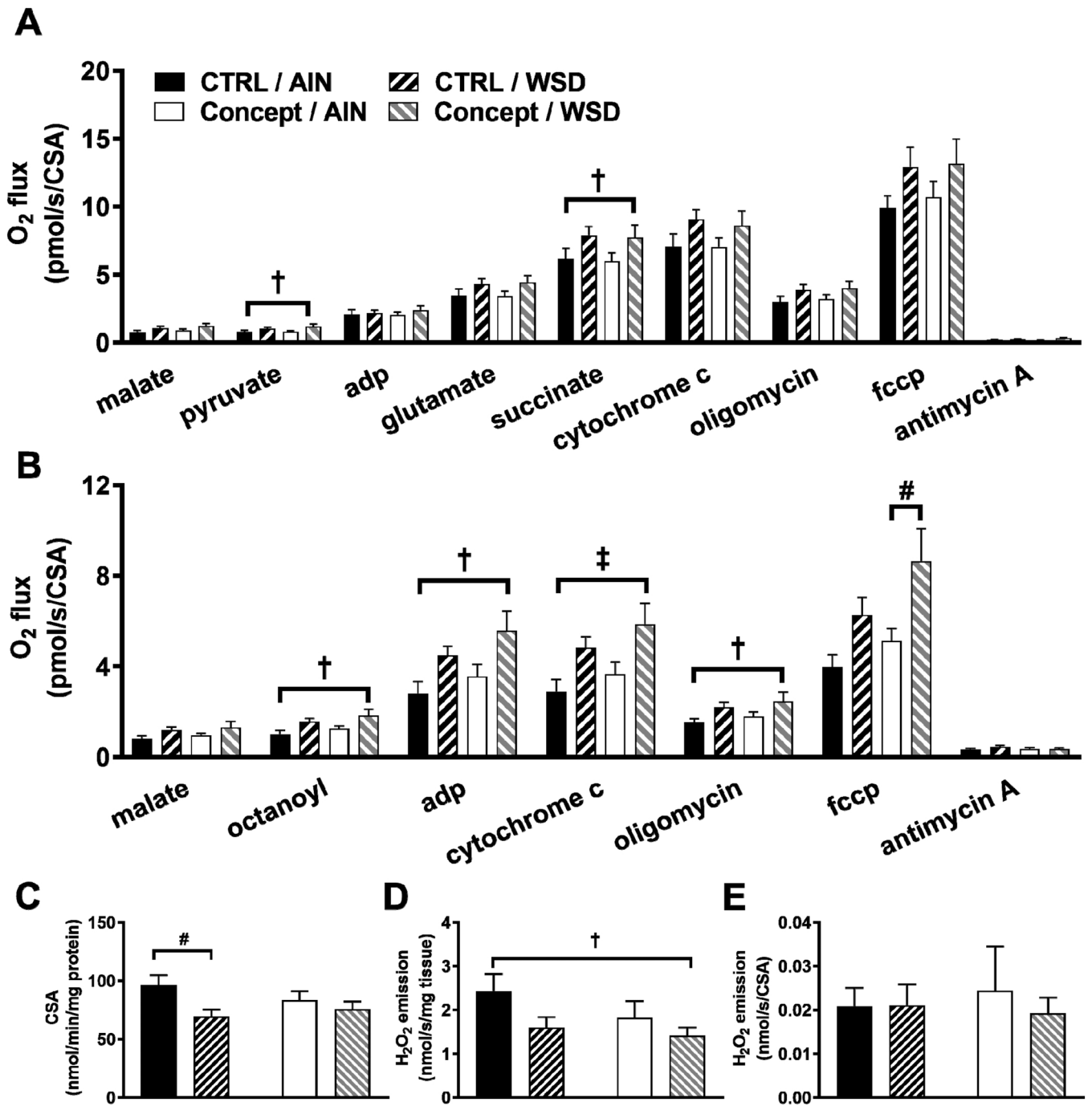

Fig. 7. Long-term effects of postnatal Concept feeding on mitochondrial function in the liver at PN98. Mitochondrial respiration [O_2 flux normalized to citrate synthase activity (CSA)] was measured with substrates supporting TCA cycle (A) and β-oxidation (B). Mitochondrial content (C) was assessed by CSA activity normalized to protein concentration. Oxidative stress was measured as the rate of malate-stimulated H_2O_2 emission and displayed per mg tissue (D) and per CSA (E). Data are shown as mean±SEM, CTRL/AIN: n = 10; CTRL/WSD: n = 12; Concept/AIN: n = 12; Concept/WSD: n = 16. Two-way ANOVA; †$p < 0.05$; ‡ $p < 0.01$ overall WSD effect; # WSD effect in groups fed the same early-life diet. AIN: American Institute of Nutrition rodent diet; CSA: citrate synthase activity, CTRL: control; cyto c: cytochrome c; fccp: carbonyl cyanide-p-trifluoromethoxyphenylhydrazone; TCA: tricarboxylic acid; WSD: western style diet.

findings point towards a protective effect of Concept in early life from WSD-induced impairment of hepatic lipid metabolism in later life [22, 23].

The long-term effects of Concept on hepatic mitochondrial respiration may result from different mechanisms. Previously, we showed that Concept increases postprandial glucose concentrations [51]. One might speculate that higher glucose levels may have stimulated TCA-cycle-linked respiration and *de novo* lipogenesis and lipid export at PN42. Subsequently, the increased β-oxidation-linked respiration in Concept/WSD at PN98 observed in the current study, may result from adaptation of hepatic mitochondria to several weeks of higher lipid exposure. Early Concept diet could thereby lead to improved handling of lipid overloads by improved "mitochondrial flexibility" for oxidation of the lipid surplus instead of storing it, supported by the observation of a lower fat mass gain in Concept/WSD.

Notably, Concept feeding did not impact skeletal muscle mitochondrial function, content or oxidative stress. Nutrient overload, induced by high-fat feeding, can result in exhaustion of adipose tissue storage

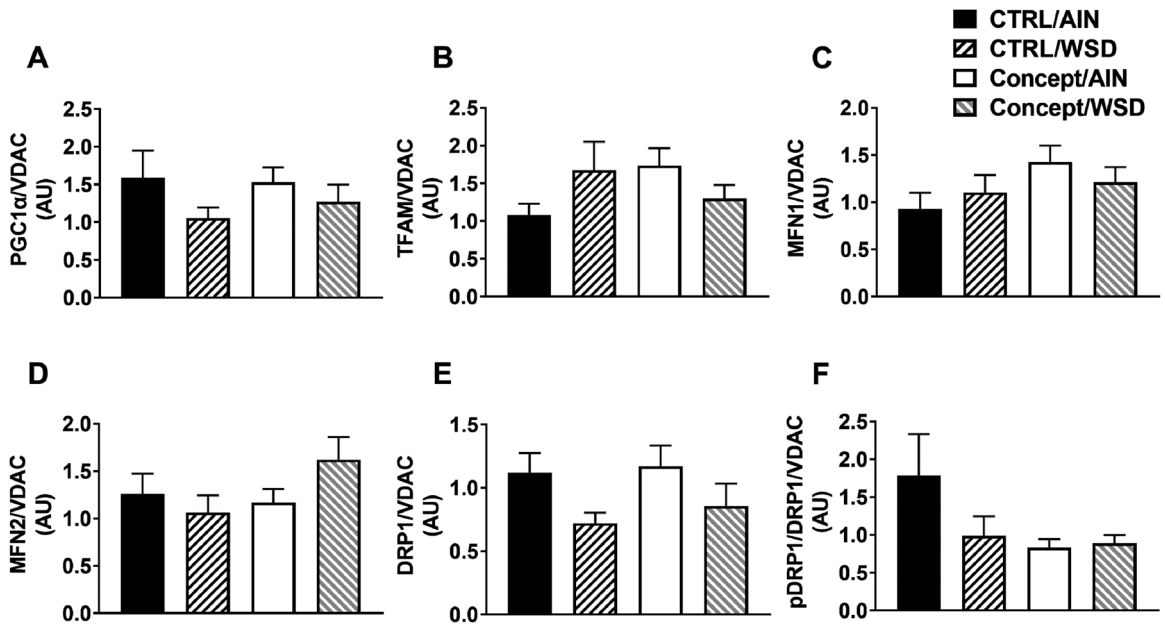

Fig. 8. Long-term effects of postnatal Concept feeding on liver-specific markers of mitochondrial biogenesis and dynamics at PN98. PGC-1α (A), TFAM (B), MFN1 (C), MFN2 (D), DRP1 (E) and pDRP1/DRP1 (F). Data are shown as mean±SEM, two-way ANOVA; CTRL/AIN: n = 10; CTRL/WSD: n = 12; Concept/AIN: n = 12; Concept/WSD: n = 14. PGC-1α: peroxisome proliferator-activated receptor gamma coactivator 1-α; TFAM: mitochondrial transcription factor A; MFN1 or 2: mitofusion protein 1 or 2; DRP1: dynamin-related protein 1, VDAC: voltage-dependent anion channel.

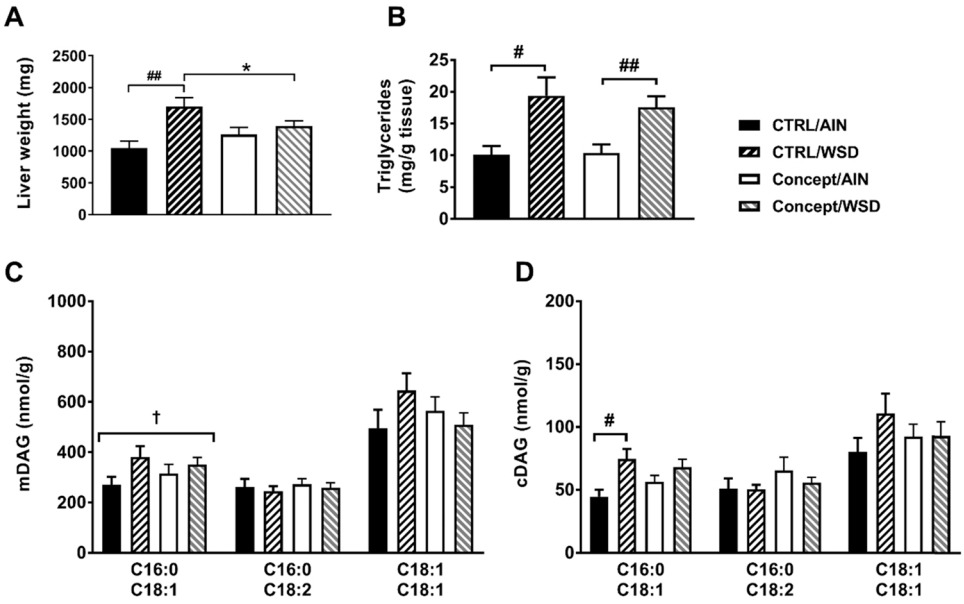

Fig. 9. Long-term effects of postnatal Concept feeding on liver weight and liver lipids on PN98. Liver weight (A), liver TG (B), mDAG (C) and cDAG (D). Data are shown as mean±SEM, CTRL/AIN: n = 10; CTRL/WSD: n = 12; Concept/AIN: n = 12 for all; Concept/WSD: n = 16 for liver weight, n = 12 for liver TG and n = 14 for mDAG and cDAG. Two-way ANOVA; †p < 0.05; overall WSD effect; # WSD effect in groups fed the same early-life diet. AIN: American institute of nutrition diet; cDAG: diacylglycerols in cytoplasm; CTRL: control; mDAG: diacylglycerols in membranes, TG: triglycerides; WSD: western style diet.

capacities and subsequent "spillover" of lipids into other tissues such as skeletal muscle or liver [52,53], potentially impairing mitochondrial function [54]. Although we cannot infer general effects of the WSD on skeletal muscle mitochondrial function, we conclude that Concept at least did not result in improved mitochondrial function in soleus muscle.

Of note, Concept feeding prevented a WSD-induced increase in mDAG and cDAG, key bioactive lipids interfering with proximal insulin signalling. Particularly, C18-containing mDAG are known to activate PKCε, which then phosphorylates threonine residues of the insulin receptor kinase and thereby impairs insulin signalling [4,55]. In contrast, sequestration of DAGs into neutral cellular lipid storage sites such as lipid droplets is considered protective towards metabolic derangements [56]. Concept feeding therefore seems to favour cellular lipid re-distribution with a profile favouring protection from hepatic insulin resistance. Moreover, the lower DAG lipid profile after Concept feeding could explain higher mitochondrial respiration, as it has recently been shown that C18-containing DAG reduced state 3 mitochondrial respiration in vitro in a dose-dependent manner [57]. In addition, to exert effects via DAGs, early life exposure to Concept feeding may cause epigenetic changes to genes involved in lipid metabolism and/or mitochondrial function as reported for body mass-induced changes in skeletal muscle and liver in humans [58,59]. Indeed, a recent study has revealed a novel role of phospholipids as a methyl sink and important regulator of histone methylation [60]. Elevated ceramides, particularly C16, C18, C22 and C24 species, have been associated with fatty liver disease and impaired mitochondrial function after feeding high-fat diets

ranging from 45% to 60% fat content [61,62]. Early life diets, mimicking human breast milk, are also naturally rich in fat (70%, see Table 1 for composition). As there are no differences regarding key metabolic outcomes (Suppl. Fig. 2), we conclude that elevated CER at this point do not associate with metabolic impairments. Furthermore, the milk phospholipid concentrate used to coat the lipid droplets in the Concept diet also contained ceramides, which may have a direct effect on ceramide levels in blood and membranes, as shown for phosphatidylcholines [63,64]. With regard to longer-term effects, it is important to note that feeding a WSD did not differentially affect CTRL or Concept mice, as shown in Suppl. Fig. 6.

Despite the significant improvements in hepatic lipid oxidation and circulating lipid peroxides, the effects of Concept on fasting glycemia, NEFA and insulin sensitivity were relatively modest. The relative short exposure to the WSD (8 weeks) may be explanatory as the effect of Concept on fasting plasma glucose, lipids, leptin, resistin and total body fat mass were more pronounced after longer (12 weeks) exposure to WSD in Concept treated mice [22]. On the other hand, exact quantification of hepatic insulin sensitivity would have required clamp tests, as HOMA-IR was assessed only upon a rather short duration of fasting (3 h), based on ethical considerations for animal well-being. Concept treated animals did respond to the obesogenic diet, but Concept feeding, even when challenged for a longer period with WSD, protected animals from development of hyperinsulinemia. Elevated plasma insulin results from higher insulin secretion or lower insulin clearance [65]. In humans, insulin clearance is not necessarily related to liver fat content [66], whereas a high-fat diet may impair insulin clearance in mice [67]. In our study, hyperinsulinemia could therefore originate from both compensatory increased insulin secretion or decreased insulin clearance. As C-peptide clearance by the liver is negligible, this parameter is used to estimate insulin secretion rate [68] or to obtain a crude measure of hepatic insulin fractional extraction from the C-peptide:insulin molar ratio [69]. However, we could not assess C-peptide in this study due to limited plasma availability.

This study has some limitations we need to address. We cannot conclude whether the effects of Concept on mitochondrial oxidative activity and lipid metabolism are due to the increased size of dietary lipid droplets, the phospholipid coating of these droplets or its combined effects. Previous studies showed, however, that both an increase in lipid droplet size and phospholipid coating are required for the phenotypic Concept effects [70]. Also monitoring of mitochondrial ATP concentration and/or synthesis, which is affected by lipid diets, diabetes and NAFLD in humans [71–73] would have been of interest, but was not possible due experimental limitations. Furthermore, to uncover subtle metabolic changes, detailed analysis of tissue-specific insulin sensitivity using hyperinsulinemic clamp tests with isotopic dilution methods [74] would be required.

In conclusion, early-life feeding with a diet containing large, phospholipid coated lipid droplets (Nuturis®) was shown to improve hepatic oxidative capacity, mitochondrial fusion and lipid profiles, directly after exposure, which persisted into later in life under an obesogenic environment in a mouse model for nutritional programming. Thus, this study highlights the role of an early life diet containing specific phospholipids mimicking human breast milk on metabolic health later in life.

Sources of support

This study was sponsored in part by Danone/Nutricia as well as by the Ministry of Culture and Science of the State of North Rhine-Westfalia (MKW NRW), the German Federal Ministry of Health (BMG) as well as by a grant of the Federal Ministry for Research (BMBF) to the German Center for Diabetes Research (DZD e. V.), the German Research Foundation (DFG, CRC 1116/2) as well as the Schmutzler-Stiftung.

Credit author statement

TJ, AK, AO, EP, EvdB and MR designed research; **TJ, AK, DP, ER, ST, LM and BD** conducted research; **TJ, AK, and ER** analysed data; **TJ, AK, DP, EP, LM, JK, EvdB and MR** interpret the data; **TJ, AK, DP and MR** wrote the paper; **MR** had primary responsibility for final content. All authors read and approved the final manuscript.

Declaration of Competing Interest

TJ: none; AK, AO: are employees of Danone Nutricia Research, EvdB: was an employee of Danone Nutricia Research at the time of the study conduct and analyses; DP none; EP: none; ER: none; BD: none; ST: none; JK: none; MR: none.

Data availability

Data supporting the conclusions of this manuscript are available upon reasonable request from the corresponding author.

Acknowledgements

Assistance: We wish to thank Ilka Rokitta and Fariba Zivehe for expert help with performing experiments and analyses, Eefje Engels for her advice for conduct of the study and Dennis Acton for contribution to data interpretation.

Grants: This study was sponsored in part by Danone Nutricia Research as well as by the Ministry of Culture and Science of the State of North Rhine-Westfalia (MKW NRW), the German Federal Ministry of Health (BMG) as well as by a grant of the Federal Ministry for Research (BMBF) to the German Center for Diabetes Research (DZD e. V.), the German Research Foundation (DFG, CRC 1116/2) as well as the Schmutzler-Stiftung. Danone Nutricia Research provided the animal diets and was involved in discussions on study design, data interpretation and writing of the manuscript.

Appendix A. Supporting information

Supplementary data associated with this article can be found in the online version at doi:10.1016/j.phrs.2022.106193.

References

[1] M. Ng, et al., Global, regional, and national prevalence of overweight and obesity in children and adults during 1980-2013: a systematic analysis for the Global Burden of Disease Study 2013, Lancet 384 (9945) (2014) 766–781.
[2] R. Sinha, et al., Prevalence of impaired glucose tolerance among children and adolescents with marked obesity, N. Engl. J. Med. 346 (11) (2002) 802–810.
[3] J.J. Reilly, J. Kelly, Long-term impact of overweight and obesity in childhood and adolescence on morbidity and premature mortality in adulthood: systematic review, Int. J. Obes. 35 (7) (2011) 891–898.
[4] M. Roden, G.I. Shulman, The integrative biology of type 2 diabetes, Nature 576 (7785) (2019) 51–60.
[5] A.P. Arruda, et al., Chronic enrichment of hepatic endoplasmic reticulum-mitochondria contact leads to mitochondrial dysfunction in obesity, Nat. Med. 20 (12) (2014) 1427–1435.
[6] S. Gancheva, et al., Interorgan metabolic crosstalk in human insulin resistance, Physiol. Rev. 98 (3) (2018) 1371–1415.
[7] T. Jelenik, et al., Mechanisms of insulin resistance in primary and secondary nonalcoholic fatty liver, Diabetes 66 (8) (2017) 2241–2253.
[8] Y.B. Lombardo, G. Hein, A. Chicco, Metabolic syndrome: effects of n-3 PUFAs on a model of dyslipidemia, insulin resistance and adiposity, Lipids 42 (5) (2007) 427–437.
[9] L.G. Gillingham, S. Harris-Janz, P.J. Jones, Dietary monounsaturated fatty acids are protective against metabolic syndrome and cardiovascular disease risk factors, Lipids 46 (3) (2011) 209–228.
[10] A. Kennedy, et al., Saturated fatty acid-mediated inflammation and insulin resistance in adipose tissue: mechanisms of action and implications, J. Nutr. 139 (1) (2009) 1–4.
[11] J.A. Oben, et al., Maternal obesity during pregnancy and lactation programs the development of offspring non-alcoholic fatty liver disease in mice, J. Hepatol. 52 (6) (2010) 913–920.

[12] A.M. Samuelsson, et al., Diet-induced obesity in female mice leads to offspring hyperphagia, adiposity, hypertension, and insulin resistance: a novel murine model of developmental programming, Hypertension 51 (2) (2008) 383–392.
[13] K.D. Bruce, et al., Maternal high-fat feeding primes steatohepatitis in adult mice offspring, involving mitochondrial dysfunction and altered lipogenesis gene expression, Hepatology 50 (6) (2009) 1796–1808.
[14] C.A. Pileggi, et al., Maternal high fat diet alters skeletal muscle mitochondrial catalytic activity in adult male rat offspring, Front Physiol. 7 (2016) 546.
[15] W. Jorgensen, et al., Changed mitochondrial function by pre- and/or postpartum diet alterations in sheep, Am. J. Physiol. Endocrinol. Metab. 297 (6) (2009) E1349–E1357.
[16] A. Oosting, et al., N-3 long-chain polyunsaturated fatty acids prevent excessive fat deposition in adulthood in a mouse model of postnatal nutritional programming, Pedia Res. 68 (6) (2010) 494–499.
[17] T. Harder, et al., Duration of breastfeeding and risk of overweight: a meta-analysis, Am. J. Epidemiol. 162 (5) (2005) 397–403.
[18] C.G. Owen, et al., Effect of infant feeding on the risk of obesity across the life course: a quantitative review of published evidence, Pediatrics 115 (5) (2005) 1367–1377.
[19] S. Gallier, et al., Using confocal laser scanning microscopy to probe the milk fat globule membrane and associated proteins, J. Agric. Food Chem. 58 (7) (2010) 4250–4257.
[20] M.C. Michalski, et al., Size distribution of fat globules in human colostrum, breast milk, and infant formula, J. Dairy Sci. 88 (6) (2005) 1927–1940.
[21] S. Gallier, et al., A novel infant milk formula concept: mimicking the human milk fat globule structure, Colloids Surf. B Biointerfaces 136 (2015) 329–339.
[22] A. Oosting, et al., Size and phospholipid coating of lipid droplets in the diet of young mice modify body fat accumulation in adulthood, Pedia Res. 72 (4) (2012) 362–369.
[23] A. Oosting, et al., Effect of dietary lipid structure in early postnatal life on mouse adipose tissue development and function in adulthood, Br. J. Nutr. 111 (2) (2014) 215–226.
[24] A. Kodde, et al., Supramolecular structure of dietary fat in early life modulates expression of markers for mitochondrial content and capacity in adipose tissue of adult mice, Nutr. Metab. 14 (2017) 37.
[25] O. Ronda, et al., Effects of an early life diet containing large phospholipid-coated lipid globules on hepatic lipid metabolism in mice, Sci. Rep. 10 (1) (2020) 16128.
[26] P.G. Reeves, F.H. Nielsen, G.C. Fahey Jr., AIN-93 purified diets for laboratory rodents: final report of the American Institute of Nutrition ad hoc writing committee on the reformulation of the AIN-76A rodent diet, J. Nutr. 123 (11) (1993) 1939–1951.
[27] J.P. Nixon, et al., Evaluation of a quantitative magnetic resonance imaging system for whole body composition analysis in rodents, Obes. (Silver Spring) 18 (8) (2010) 1652–1659.
[28] D. Pesta, E. Gnaiger, High-resolution respirometry: OXPHOS protocols for human cells and permeabilized fibers from small biopsies of human muscle, Methods Mol. Biol. 810 (2012) 25–58.
[29] C. Koliaki, et al., Adaptation of hepatic mitochondrial function in humans with non-alcoholic fatty liver is lost in steatohepatitis, Cell Metab. 21 (5) (2015) 739–746.
[30] C. Doerrier, et al., High-resolution FluoRespirometry and OXPHOS protocols for human cells, permeabilized fibers from small biopsies of muscle, and isolated mitochondria, Methods Mol. Biol. 1782 (2018) 31–70.
[31] T. Jelenik, et al., Insulin resistance and vulnerability to cardiac ischemia, Diabetes 67 (12) (2018) 2695–2702.
[32] C. Preuss, et al., A new targeted lipidomics approach reveals lipid droplets in liver, muscle and heart as a repository for diacylglycerol and ceramide species in non-alcoholic fatty liver, Cells 8 (3) (2019).
[33] J. Folch, M. Lees, G.H. Sloane Stanley, A simple method for the isolation and purification of total lipides from animal tissues. J. Biol. Chem. 226 (1) (1957) 497–509.
[34] M. Apostolopoulou, et al., Metabolic responsiveness to training depends on insulin sensitivity and protein content of exosomes in insulin-resistant males, Sci. Adv. 7 (41) (2021) eabi9551.
[35] K.J. Livak, T.D. Schmittgen, Analysis of relative gene expression data using real-time quantitative PCR and the 2(-Delta Delta C(T)) Method, Methods 25 (4) (2001) 402–408.
[36] S.M. Haffner, H. Miettinen, M.P. Stern, The homeostasis model in the San Antonio Heart Study, Diabetes Care 20 (7) (1997) 1087–1092.
[37] Q. Tang, et al., Optimal cut-off values for the homeostasis model assessment of insulin resistance (HOMA-IR) and pre-diabetes screening: developments in research and prospects for the future, Drug Disco Ther. 9 (6) (2015) 380–385.
[38] B. Cannon, J. Nedergaard, Nonshivering thermogenesis and its adequate measurement in metabolic studies, J. Exp. Biol. 214 (Pt 2) (2011) 242–253.
[39] Z. Wang, et al., Evaluation of specific metabolic rates of major organs and tissues: comparison between nonobese and obese women, Obes. (Silver Spring) 20 (1) (2012) 95–100.
[40] G. Mingrone, et al., Influence of maternal obesity on insulin sensitivity and secretion in offspring, Diabetes Care 31 (9) (2008) 1872–1876.
[41] N. Modi, et al., The influence of maternal body mass index on infant adiposity and hepatic lipid content, Pedia Res. 70 (3) (2011) 287–291.
[42] V. Nobili, et al., A protective effect of breastfeeding on the progression of non-alcoholic fatty liver disease, Arch. Dis. Child 94 (10) (2009) 801–805.
[43] J. Liu, et al., Effects of intrauterine growth retardation and maternal folic acid supplementation on hepatic mitochondrial function and gene expression in piglets, Arch. Anim. Nutr. 66 (5) (2012) 357–371.
[44] S.J. Borengasser, et al., Maternal obesity during gestation impairs fatty acid oxidation and mitochondrial SIRT3 expression in rat offspring at weaning, PLoS One 6 (8) (2011), e24068.
[45] R.D. Sheldon, et al., eNOS deletion impairs mitochondrial quality control and exacerbates Western diet-induced NASH, Am. J. Physiol. Endocrinol. Metab. 317 (4) (2019) E605–E616.
[46] C.H. Yao, et al., Mitochondrial fusion supports increased oxidative phosphorylation during cell proliferation, Elife 8 (2019).
[47] C.A. Galloway, et al., Decreasing mitochondrial fission alleviates hepatic steatosis in a murine model of nonalcoholic fatty liver disease, Am. J. Physiol. Gastrointest. liver Physiol. 307 (6) (2014) G632–G641.
[48] L. Wang, et al., Disruption of mitochondrial fission in the liver protects mice from diet-induced obesity and metabolic deterioration, Diabetologia 58 (10) (2015) 2371–2380.
[49] Y. Wang, et al., Reducing embryonic mtDNA copy number alters epigenetic profile of key hepatic lipolytic genes and causes abnormal lipid accumulation in adult mice, Febs J. 288 (23) (2021) 6828–6843.
[50] S. Gallier, et al., A novel infant milk formula concept: mimicking the human milk fat globule structure, Colloids Surf. B: Biointerfaces 136 (2015) 329–339.
[51] S. Baumgartner, et al., Infant milk fat droplet size and coating affect postprandial responses in healthy adult men: a proof-of-concept study, Eur. J. Clin. Nutr. 71 (9) (2017) 1108–1113.
[52] T. Sarabhai, et al., Dietary palmitate and oleate differently modulate insulin sensitivity in human skeletal muscle, Diabetologia (2021).
[53] A. Lettner, M. Roden, Ectopic fat and insulin resistance, Curr. Diab Rep. 8 (3) (2008) 185–191.
[54] C. Koliaki, M. Roden, Alterations of mitochondrial function and insulin sensitivity in human obesity and diabetes mellitus, Annu Rev. Nutr. 36 (2016) 337–367.
[55] K. Lyu, et al., A membrane-bound diacylglycerol species induces PKCε-mediated hepatic insulin resistance, Cell Metab. 32 (4) (2020) 654–664.e5.
[56] J.L. Cantley, et al., CGI-58 knockdown sequesters diacylglycerols in lipid droplets/ER-preventing diacylglycerol-mediated hepatic insulin resistance, Proc. Natl. Acad. Sci. USA 110 (5) (2013) 1869–1874.
[57] L. Perreault, et al., Intracellular localization of diacylglycerols and sphingolipids influences insulin sensitivity and mitochondrial function in human skeletal muscle, JCI Insight 3 (3) (2018).
[58] S. Gancheva, et al., Dynamic changes of muscle insulin sensitivity after metabolic surgery, Nat. Commun. 10 (1) (2019) 4179.
[59] M. Ahrens, et al., DNA methylation analysis in nonalcoholic fatty liver disease suggests distinct disease-specific and remodeling signatures after bariatric surgery, Cell Metab. 18 (2) (2013) 296–302.
[60] C. Ye, et al., A metabolic function for phospholipid and histone methylation, Mol. Cell 66 (2) (2017) 180–193 e8.
[61] A. Zalewska, et al., High-fat diet affects ceramide content, disturbs mitochondrial redox balance, and induces apoptosis in the submandibular glands of mice, Biomolecules 9 (12) (2019) 877.
[62] T. Kasumov, et al., Ceramide as a mediator of non-alcoholic Fatty liver disease and associated atherosclerosis, PLoS One 10 (5) (2015), e0126910.
[63] X. He, et al., Metabolic phenotype of breast-fed infants, and infants fed standard formula or bovine MFGM supplemented formula: a randomized controlled trial, Sci. Rep. 9 (1) (2019) 339.
[64] A. Kodde, et al., The effect of dietary lipid quality in early life on serum LysoPC(18:2) levels and their association with adult blood glucose levels in intrauterine growth restricted rats, Nutr. Metab. 18 (1) (2021) 101.
[65] S.H. Jung, et al., Adapting to insulin resistance in obesity: role of insulin secretion and clearance, Diabetologia 61 (3) (2018) 681–687.
[66] K.M. Utzschneider, S.E. Kahn, D.C. Polidori, Hepatic insulin extraction in NAFLD is related to insulin resistance rather than liver fat content, J. Clin. Endocrinol. Metab. 104 (5) (2019) 1855–1865.
[67] K.P. Foley, et al., Gut microbiota impairs insulin clearance in obese mice, Mol. Metab. 42 (2020), 101067.
[68] E. Van Cauter, et al., Estimation of insulin secretion rates from C-peptide levels. Comparison of individual and standard kinetic parameters for C-peptide clearance, Diabetes 41 (3) (1992) 368–377.
[69] M.R. Lebowitz, S.A. Blumenthal, The molar ratio of insulin to C-peptide. An aid to the diagnosis of hypoglycemia due to surreptitious (or inadvertent) insulin administration, Arch. Intern. Med. 153 (5) (1993) 650–655.
[70] A. Baars, et al., Milk fat globule membrane coating of large lipid droplets in the diet of young mice prevents body fat accumulation in adulthood, Br. J. Nutr. 115 (11) (2016) 1930–1937.
[71] T. Sarabhai, et al., Monounsaturated fat rapidly induces hepatic gluconeogenesis and whole-body insulin resistance, JCI Insight 5 (10) (2020).
[72] Y. Kupriyanova, et al., Early changes in hepatic energy metabolism and lipid content in recent-onset type 1 and 2 diabetes mellitus, J. Hepatol. 74 (5) (2021) 1028–1037.
[73] A.I. Schmid, et al., Liver ATP synthesis is lower and relates to insulin sensitivity in patients with type 2 diabetes, Diabetes Care 34 (2) (2011) 448–453.
[74] K. Philippaert, et al., Bax inhibitor-1 deficiency leads to obesity by increasing Ca(2+)-dependent insulin secretion, J. Mol. Med. 98 (6) (2020) 849–862.